Marine and Petroleum Geology 25 (2008) 791–803

Contents lists available at ScienceDirect

Marine and Petroleum Geology

journal homepage: www.elsevier.com/locate/marpetgeo

Reverse structures in accommodation zone and early compartmentalization of extensional system, Laminaria High (NW shelf, Australia)

Laurent Langhi [a,b,*], Gilles D. Borel [c]

[a] Institute of Geology and Palaeontology, University of Lausanne, CH-1015 Lausanne, Switzerland
[b] CSIRO Petroleum, ARRC, Technology Park, 26 Dick Perry Avenue, Kensington, WA 6151, Australia
[c] Museum of Geology, Lausanne, UNIL, CH-1015 Lausanne, Switzerland

ARTICLE INFO

Article history:
Received 6 February 2007
Received in revised form 2 October 2007
Accepted 4 October 2007

Keywords:
Accommodation zone
Flower structure
Australia
Seismic attributes

ABSTRACT

The sediments dynamics and structural development associated with the Late Jurassic rifting phase represent the key factors on the accumulation of hydrocarbon in the Timor Sea. On the Laminaria High (Bonaparte Basin) the main Oxfordian–Kimmeridgian E–W fault system forms structural traps where several discoveries have been made.

Recent 3D seismic analysis has been performed based on a combination of classic structural analysis, structure-sensitive seismic attributes (grid-based, surface-based, full-volume) and meta-attribute computations. The analysis has revealed secondary reverse structures associated with the main E–W fabric and prone to act as secondary hydrocarbon traps and/or as migration barriers.

The main E–W fault system consists of a complex series of sub-parallel faults that connect via relay ramps or accommodation zones. One of these zones is associated with a transverse anticline resulting from the development of a positive flower structure.

The model presented in this article and supported by the interpretation of the seismic data demonstrates that the flower structure developed in an extensional setting. The formation of such a reverse structure can be related to the propagation process of the main E–W fault plane which grows by addition of secondary en-echelon tip faults. Isopach analysis and displacement pattern suggest that a zone of differential displacement occurs between two segments of the main fault plane, inducing local strike-slip movements able to form transpressional uplift associated with restraining bend.

This structure related to a rotation of the stress field compartmentalises the early development of the adjacent graben and then controls the distribution of the syn-rift Frigate Fm (Oxfordian–Kimmeridgian).

1. Introduction

The Mesozoic extensional event that culminated with the Late Jurassic Argo Abyssal Plain opening (Müller et al., 1998; Borel and Stampfli, 2002) is mainly responsible for the general NE–SW structural grain that characterise the present day Australian NW Shelf.

Due to older structures related to rifting episodes during the Devonian–Carboniferous (Baillie et al., 1994) and the Permo-Carboniferous (Etheridge and O'Brien, 1994; Borel and Stampfli, 2002; Langhi and Borel, 2005) such a trend can locally vary as it is the case on the Laminaria High and the Nancar Trough area (Bonaparte Basin) where major Mesozoic structures are E–W trending (de Ruig et al., 2000; Castillo et al., 2000).

In this area, the development of basinward and landward dipping normal faults post-date the deposition of the Laminaria Fm during the Callovian–Oxfordian and form a series of horsts and grabens.

Previous studies (Smith et al., 1996; de Ruig et al., 2000) have described the Late Jurassic structures of the Laminaria High and the Nancar Trough area, focussing mainly on the structural highs where hydrocarbon discoveries have been made within the Callovian–Oxfordian sandstones (Longley et al., 2002).

Further detailed 3D investigation on this area highlights the complex and segmented structure of the main E–W Mesozoic normal fault systems.

Furthermore, seismic attribute analysis performed on the Late Jurassic–Early Cretaceous section reveals secondary oblique structural trends (NW- to NNW-trending) mainly located within the main depressions. These trends represent accommodation zones (Faulds and Varga, 1998) used to transfer displacement and elevation between loci of differential deformation.

Thorough 3D seismic analysis and seismic attribute mapping of such a structural feature located on the western part of the Laminaria 3D survey reveal the presence of a reverse faults system

* Corresponding author. Tel.: +61 (0)8 6436 8741; fax: +61 (0)8 6436 8555.
E-mail address: laurent.langhi@csiro.au (L. Langhi).

0264-8172/$ – see front matter Crown Copyright © 2008 Published by Elsevier Ltd. All rights reserved.
doi:10.1016/j.marpetgeo.2008.04.007

forming a positive flower structure and compartmentalizing an E–W trending graben.

This paper presents elements and model those explain and reconcile the presence of an oblique flower structure in extensional setting and that link its development to the propagation process of the main EW border fault system.

2. Structural and stratigraphic setting

The study area is located on the Laminaria High (Fig. 1), in the Northern Bonaparte Basin. It lies on the boundary between the continental shelf and slope that plunges to the north into the Timor Trough. It is regionally bounded by the Nancar and Cartier Troughs to the south and the Flamingo Syncline to the east. Smith et al. (1996) defined the Laminaria High as a small, east-orientated drowned platform-remnant with a shallow Palaeozoic basement relative to the adjacent synclines.

The Bonaparte Basin has a complex structural history and presents Palaeozoic and Mesozoic sub-basins and drowned platforms that can exhibit strongly divergent orientations.

The Phanerozoic tectonostratigraphic evolution of the Bonaparte Basin has been documented by Veevers (1988), Pattillo and Nicholls (1990), AGSO (1994), Baillie et al. (1994), Hocking et al. (1994), Whittam et al. (1996), O'Brien et al. (1996), Shuster et al. (1998), Labutis et al. (1998), O'Brien et al. (1999) or Longley et al. (2002).

Three major extensional phases have affected the Bonaparte Basin during the Phanerozoic.

- On the southern part of the basin a localised evaporite deposition during the Ordovician–Silurian was followed by an initial phase of rifting associated with the Late Devonian–Early Carboniferous development of the NW-trending Petrel Sub-basin. Although Early Palaeozoic deposits are generally too deep to be observed on seismic in the Northern Bonaparte Basin (de Ruig et al., 2000), the NW–SE fabric associated with this episode can be recognised in the broad NW–SE trend of the Nancar Trough, Sahul Syncline and Flamingo Syncline.

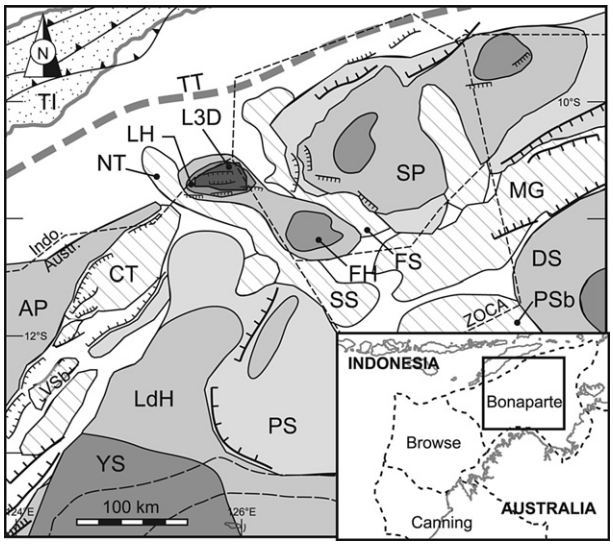

Fig. 1. Geological setting and Late Jurassic structural elements of the Laminaria High. AP: Ashmore Platform; CT: Cartier Trough; DS: Darwin Shelf; FH: Flamingo High; FS: Flamingo Syncline; L3D: Laminaria 3D survey; LdH: Londonderry High; LH: Laminaria High; MG: Malita Graben; NT: Nancar Trough, PSb: Petrel Sub-basin; PS: Plover Shelf; SP: Sahul Platform; SS Sahul Syncline; TI: Timor Island; TT: Timor Trough; VSb: Vulcan Sub-basin; YS: Yampi Shelf.

- The Permo-Carboniferous is marked by the initiation of the Neotethys rift system that propagated from Australia to the eastern Mediterranean area, removing slivers of Gondwana terranes (Borel and Stampfli, 2002; Stampfli and Borel, 2002). On the northwestern margin of Australia, this rifting generated extensive deformation trending mainly northeast (Langhi and Borel, 2005) that defined the large-scale geometry of the margin and that formed the so-called Westralian Superbasin (Yeates et al., 1987).
- Superimposed on this Palaeozoic structural grain is a regional Late Jurassic NE–SW fabric (de Ruig et al., 2000), which is related to the final break-up of Gondwana and the opening of the abyssal plains (AGSO, 1994). In the Bonaparte Basin, the NE-trending Vulcan Sub-basin and Cartier Trough as well as the Malita Graben highlight this structural fabric. On the Laminaria High, this NE–SW trend changes to E–W (de Ruig et al., 2000). This variation could be attributed to the presence of underlying structures.

Following the continental break-up a classic passive margin sequence developed on the NW Shelf, which gave way throughout the Tertiary to a carbonate shelf (e.g. Whittam et al., 1996).

During the Miocene–Pleistocene the convergence of the Australian Plate and the Banda Arc established an oblique collisional setting in the northern Bonaparte Basin (Keep et al., 2002). Although strike-slip reactivation has been suggested in the Timor Sea (e.g. Shuster et al., 1998) local studies in the Northern Bonaparte Basin (Harrowfield et al., 2003) and the Laminaria High (de Ruig et al., 2000; Langhi, 2006) continuously report Neogene net normal fault offsets, while structural patterns typically associated with strike-slip movement are often lacking. Furthermore, on the basis of the regional structural trend and paleo-stress estimation using fault-slip inversion technique, Gartrell and Lisk (2005) and Gartrell et al. (2006) have suggested a north–north-west extensional regime associated with the late Miocene in the Timor Sea. Langhi (2006) suggests that the tension induced by the flexure of the Australian margin may be a major local factor for the development of the Neogene structures.

The lateral distribution of the Neogene strain is primarily inherited from the pre-existing Jurassic architecture (Gartrell et al., 2006) with most of the deformation accommodated within the Tertiary section by newly formed Miocene–Pliocene normal fault systems (Langhi, 2006).

The deposits of the Laminaria High clearly record the Mesozoic rifting phase (Fig. 2).

The deltaic and shelfal marine Plover Fm (Labutis et al., 1998) spans most of the Early and Middle Jurassic. Deltaic and shelfal marine environment still characterises the Callovian–Oxfordian with the deposition of the Laminaria sandstones (Table 1). This period is coeval with a major regional uplift (J30 sequence in Longley et al., 2002) that marks the transition between the pre-rift and syn-rift phases. During that period, the northern part of the Kimberley Craton acted as the major sediment source (de Ruig et al., 2000).

The subsequent formations clearly reflect a deepening of the depositional environment with the presence of the Frigate (Oxfordian–Kimmeridgian), Flamingo (Tithonian–Berriasian) and Echuca Shoals (Valanginian–Barremian) shaly formations, characteristic of open marine environment (Whittam et al., 1996). The thickness variation recorded in several wells (Table 1) suggests that the Frigate and Flamingo Formations are coeval with the main rift-related fault displacement phase. This section, associated with a rapid rise in relative sea level, represents the base of the regional seal. Additionally the Oxfordian–Berriasian shales (e.g. Frigate and Flamingo Fm) are traditionally considered to contain the principal oil-prone source-rock in the region.

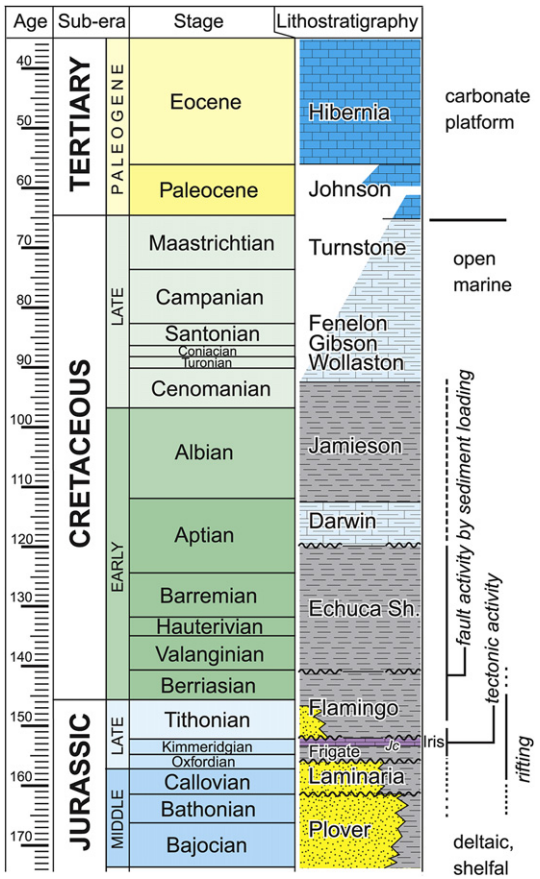

Fig. 2. Late Mesozoic and Early Cainozoic lithostratigraphy for the Laminaria High (modified from de Ruig et al., 2000).

The Aptian–Maastrichian sequence is composed of northwesterly-thinning progradational wedges, similar to those found elsewhere in the Bonaparte Basin. It comprises the Darwin, Jamieson, Woolaston, Gibson, Fenelon and Turnston Fms. These Cretaceous sediments are thin compared to the adjacent areas and substantial erosion and non-deposition occurred over the Laminaria High (Smith et al., 1996).

The overlying thick Cainozoic section represents an extensive cover of shelfal carbonates prograding over the Northern Bonaparte Basin.

3. Methods, 3D interpretation workflow

Seismic data available for this study comprises the Laminaria 3D survey with asymmetric binning of 12.5 m × 25 m. It is characterised by an average signal-to-noise ratio for the Late Jurassic–Early Cretaceous section partly due to low reflectivity at top reservoir (Smith et al., 1996). Therefore, several workflows have been used to combine seismic attributes and known classification processes into enhanced seismic resolution (Reymond, 2000; Langhi and Reymond, 2005).

The structural interpretation is essentially based on the recognition of geological features observed along various surfaces (surface-based and grid-based attributes on interpreted horizon or regional paleotrend horizons) and on vertical seismic sections. The computation and analysis of full attribute cubes increase the number of independent representations of geobodies and further constrain the recognition of the structural patterns and the mapping of their lateral extent. A final important step in the interpretation workflow consisted of iterating between the grid-based and the section-based results to validate the geological interpretations.

This approach has been applied to improve the seismic recognition of the Late Jurassic structural style and has led to a better recognition of major and subtle fault systems and to an extended characterisation of the local structural evolution.

3.1. Structural geobodies

Unlike "sedimentary" geobodies (e.g. fan, channel, sand sheet) that can be defined by their internal reflectivity and seismic texture (Langhi and Reymond, 2005), faults do not generally show characteristic internal texture in classical seismic representation (e.g. amplitude, phase or frequency). These structural features represent special type of seismic geobodies more likely to appear like trends and are characterised by the variation or the discontinuity of the seismic signal at their boundaries. Such variation of the seismic signal can be captured on map by selected sets of grid-based and surface-based seismic attributes (e.g. instantaneous attributes mapping the values of any transform of the seismic trace along a surface trend or integrated attributes from a defined volume restricted around the surface, see below). The definition of the local variance has been used in order to extract the unconformity of the seismic signal. Variance cubes were computed (regional, EW- and NS-trending variance cubes) in order to track specific structural orientations and provided independent input towards 3D seismic structural interpretation.

Table 1
Stratigraphy for the Late Jurassic–Early Cretaceous on the Laminaria High

Horizon	Vidalia-1			Pandorina-1			Corallina-1		
	Age	Depth (mRT)	Litho	Age	Depth (mRT)	Litho	Age	Depth (mRT)	Litho
Top Echuca Shoals Fm (KA)	Barremian–Aptian	2948	Clst, calc clst	Barremian–Aptian	3020	Clst	Barremian–Aptian	2924	Clst
Echuca Shoals Fm thickness		36			42			26	
Top Flamingo Fm (KV)	Berriasian	2984	Clst	Haut	3062	Clst	Berriasian	2950	Clst, silty clst
Flamingo Fm thickness		109			197			172	
Near top Frigate Fm (Jc this study)	Oxfordian–Tithonian	3093	Cist	Tithonian	3259	Clst, minor sltst	Oxfordian–Tithonian	3122	Silty clst
Frigate Fm thickness		26			76			42	
Top Laminaria Fm	Callovian–Oxfordian	3119	Sst, minor sltst, clst	Callovian–Oxfordian	3335	Sst, minor sltst, clst	Oxfordian	3164	Sst, minor clst
Laminaria Fm thickness		79			81			120	
Top Plover Fm	Callovian	3198	Sst, minor sltst, clst	Callovian	3416	Sst, minor sltst, clst	Callovian	3284	Sst, sltst

Vidalia-1, Pandorina-1 and Corallina-1 record the deposition history on the three main structural features of the study area, respectively, the H1horst, the G1 graben and the H2 horst (see Fig. 3). Note the thickening of the Frigate Fm in Pandorina-1 suggesting that the Oxfordian–Kimmeridgian is coeval with the main rift-related fault displacement phase. Sst = sandstone; sltst = siltstone; clst = claystone.

3.2. Seismic attributes

For this research, following pre-conditioning of the data by post-stack filtering, the following seismic attributes have been successfully combined to capture and map structural geobodies distribution.

- Seismic attributes derived from variance cubes computed along paleo-horizons or along interpreted horizons (or restricted volume around them, i.e. integrated attributes). It includes amplitude extraction, apparent polarity and the reflection strength. They were used to define the structural geobodies and their geometry. Seismic attributes derived from

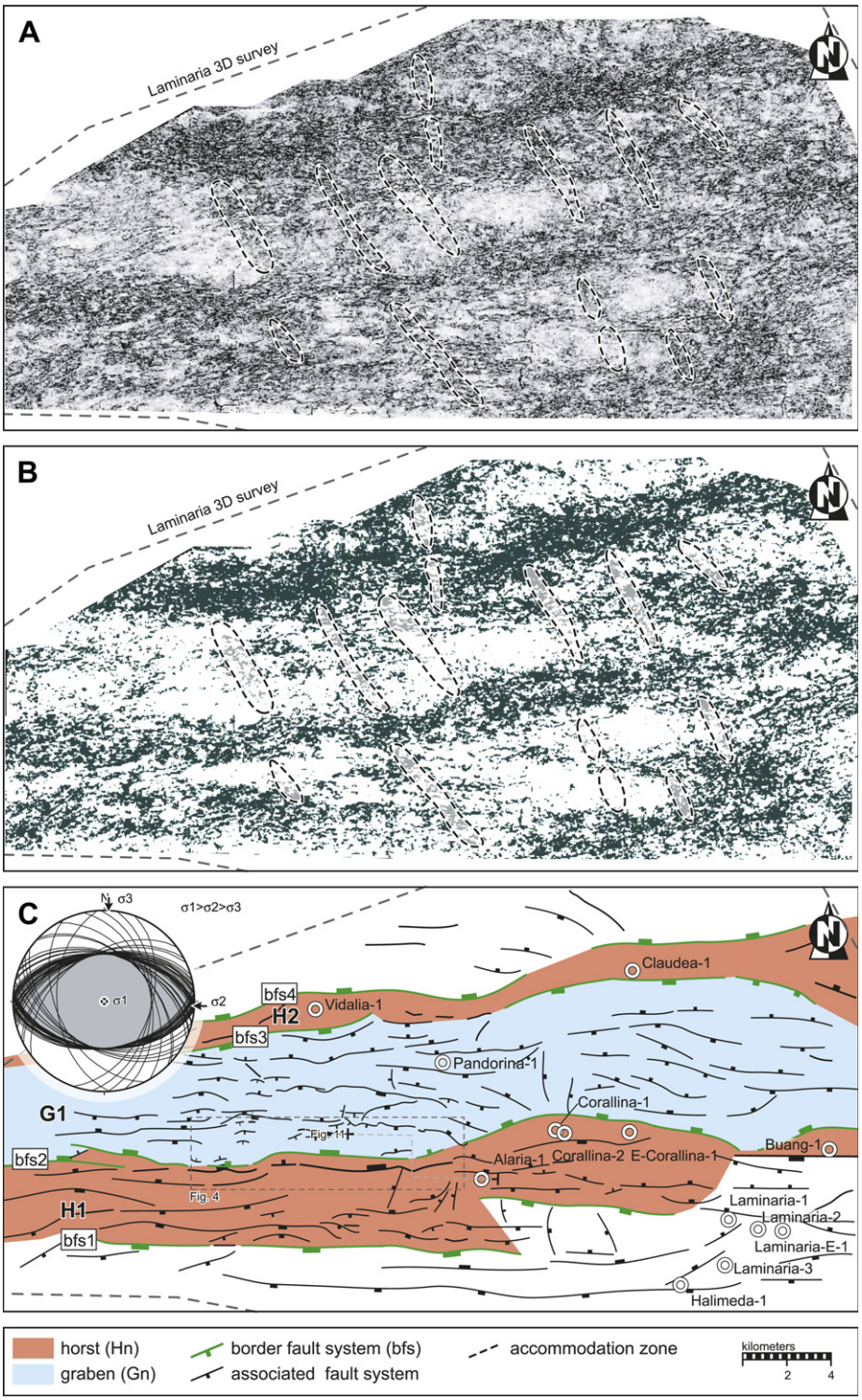

Fig. 3. Late Jurassic–Early Cretaceous structure map on the Laminaria High based on a paleo-horizon. (A) Correlation map highlighting the principal EW-trending fault systems and an oblique (NW–NNW) structural trend related to accommodation zones. Coherent zones in light gray. (B) Meta-attribute enhancing the definition of the structural trends, some characteristics of the accommodation zones are preserved. Structural features in black. (C) Structure map and definition of the principal border fault systems and the main horsts (H1 and H2) and graben (G1). The local Late Jurassic stress field for the Laminaria High is characteristic of an extensional regime with $\sigma_v > \sigma_{hmax} > \sigma_{hmin}$ ($\sigma_1 > \sigma_2 > \sigma_3$).

the spectral decomposition of the reflectivity response on variance cubes are used to approximate and laterally interpolate the extent of geobodies.
- Seismic attributes related to signal continuity computed along paleo-horizons or interpreted horizons (or restricted volume around) and derived from the original seismic amplitude version: instantaneous phase, integrated cosine of phase and correlation maps (Fig. 3). They were used to constrain the geometry of structural geobodies. The apparent polarity and the reflection strength can also guide the delimitation of structural features.
- Grid-based attributes related to the geometry of interpreted grid (no amplitude data used): dip, azimuth and edge enhancement. They were used to refine the interpretation of main structural features and to define subtle fracture systems.

3.3. Enhancing seismic attributes resolution

Three processes have been applied to improve the limited resolution observed within each seismic attribute.

- Meta-attributes (de Rooij and Tingdahl, 2002) or mathematical combinations of seismic attribute (Langhi and Reymond, 2005) to increase continuity-related anomalies in a low-resolution environment. While attributes' classification methods (see below) relies on the statistical recognition of a "seismic identity" of a geobody, the definition of meta-attributes is based, for this research, on independent representations of a common character that are normalized and mathematically combined in order to enhance the signal-to-noise ratio (e.g. see Fig. 3b).
- Geostatistical classification methods to optimise the identification and outlines of structural geobodies at both local and regional scales. Due to the lack of calibration data for structural features an unsupervised approach has been used.
- Neural network based classification algorithms (also unsupervised).

4. Results

The Phanerozoic structural style of the Laminaria High reflects its tectonic history and is composed of three levels with a Permian block-faulted structural *basement*, a Jurassic–Cretaceous horst and graben system and a Late Cainozoic system (de Ruig et al., 2000).

A series of EW-trending principal border fault systems (bfs, Fig. 3) characterises the Jurassic–Cretaceous structural level and delimits the main horsts and grabens (H1, H2 and G1, Fig. 3). These fault systems often consist of a series of multiple sub-parallel fault planes that connect via relay ramp or accommodation zones, assisting the distribution and accommodation of most of the overall strain.

The geometry and distribution of the principal border faults have been used to determinate the local Late Jurassic stress field at the Laminaria High (Fig. 3). The regime appears as purely extensional with the maximum stress (σ_1), vertical and minimum stress (σ_3), horizontal and parallel to the extension direction at 3N

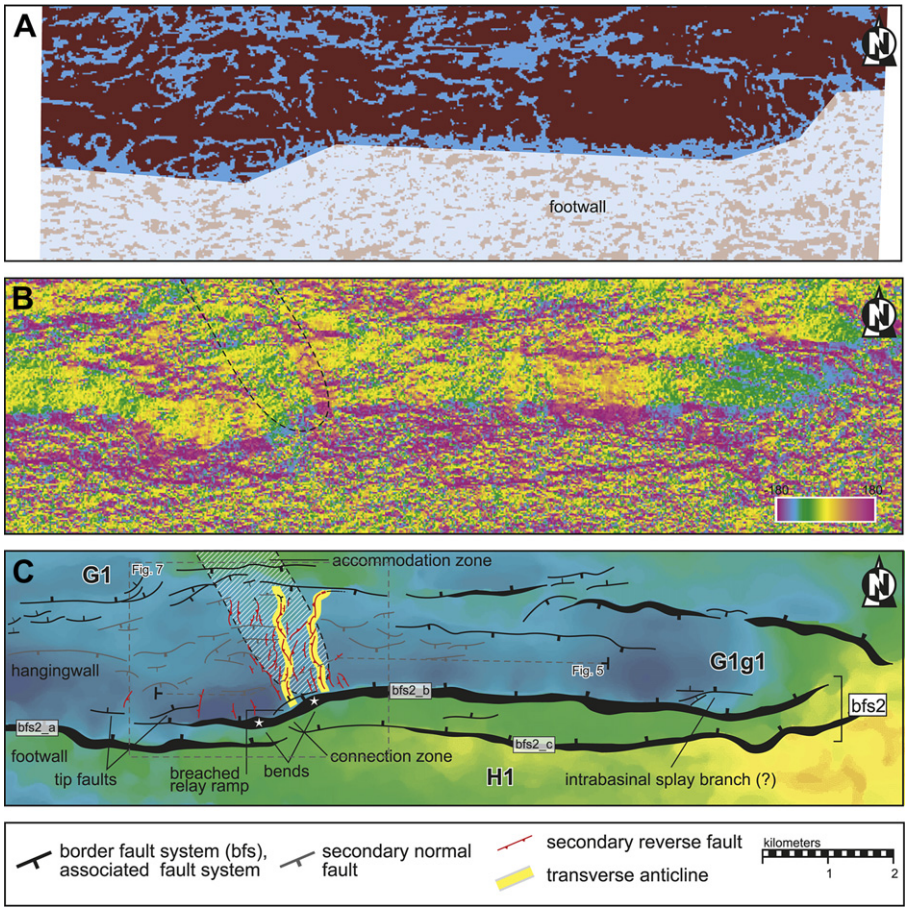

Fig. 4. Late Jurassic structure map on the western Laminaria High, top Laminaria Fm. Location of Fig. 3. (A) Structural class map with fault zone in light gray (2 classes, unsupervised neural network based classification). (B) Azimuth map, top Laminaria Fm. (C) Structure map on the top Laminaria Fm, distribution of secondary systems associated with the border fault system bfs2. Low areas in dark gray, high areas in light gray.

(Fig. 3). This orientation is slightly oblique to the regional extensional direction inferred by either AGSO (1994) or Müller et al. (1998) based upon magnetic anomalies definition. This variation could most likely be related to the presence of underlying inherited structures affecting the development of the Jurassic–Cretaceous fault systems.

The individual fault planes of the principal border fault systems (Figs. 3 and 4) often display undulating fault strike geometry, typical of relict connection zones (Fig. 4) between fault segments (Marchal, 1998; Marchal et al., 2003).

A major seaward (northward) dipping border fault system (bfs2, Fig. 3) characterises the Late Jurassic structure on the study area and delimits a southern positive structural trend, the location of the Corallina and Laminaria fields (H1, Fig. 3), and a northern major graben (G1, Fig. 3). The latter is bounded, to the north, by a narrow horst where Vidalia-1 and Claudea-1 have been drilled (H2, Fig. 3). This fault system (bfs2, Figs. 3 and 4) includes a series of main fault planes with an average length of ca. 10 km that display several associated features such as fault tips, breached relay ramp and possible splay branch as well as bends (e.g. fault bfs2_b, Fig. 4).

Beside the principal fault systems, associated fault systems (also EW-trending) are well developed and help to accommodate the Late Jurassic strain (Figs. 3 and 4). The associated fault strike (Fig. 4) also displays undulating or completely segmented geometry. Relay ramps are also visible as well as rapid inversion of dip (Fig. 4). These systems are particularly well developed within the main graben (G1, Figs. 3 and 4) where they form several associated restricted horsts and grabens (e.g. G1g1, Fig. 4).

Seismic attributes generated on a paleo-horizontal through the Jurassic–Cretaceous structural level show the E–W trend for the principal border faults and the associated fault systems. These attributes also reveal subtle trends, obliquely orientated (NW–NNW) to the principal trend (Fig. 3). The latter structural features coincide with accommodation zones (Faulds and Varga, 1998) that developed to transfer displacement and elevation between loci of differential deformation. They correspond to belts of overlapping fault terminations well known in rift setting (e.g. Morley et al., 1990; Morley, 2002; Moustafa, 2002).

3D seismic interpretation reveals that such an accommodation zone, located on the western part of the study area, is formed by a transverse anticline (Figs. 4 and 5). This structure is related to a connection zone (undulation) between segments of a principal seaward dipping fault (bfs2_b, Fig. 4) and compartmentalises the associated restricted graben that is intersected (i.e. G1g1, Fig 4).

Similar secondary structures that develop obliquely to the principal border faults have been reported in rift and extensional settings in the Red Sea (Moustafa, 2002) in East Africa (Morley, 2002), in Eastern North America (Schlische, 1993) or in the Alpine Briançonnais domain (Borel, 1997).

Thorough interpretation and attributes' analysis in the vicinity of the transverse anticline (Figs. 4 and 6) reveals that this feature is the result of the development of a series of reverse faults forming a positive flower structure (Figs. 5 and 7).

In map view, the flower structure is characterised by an anastomosing array of reverse faults (Fig. 6) that forms anticline "pop-up" structures (domal uplift, see Stone, 1995). These display

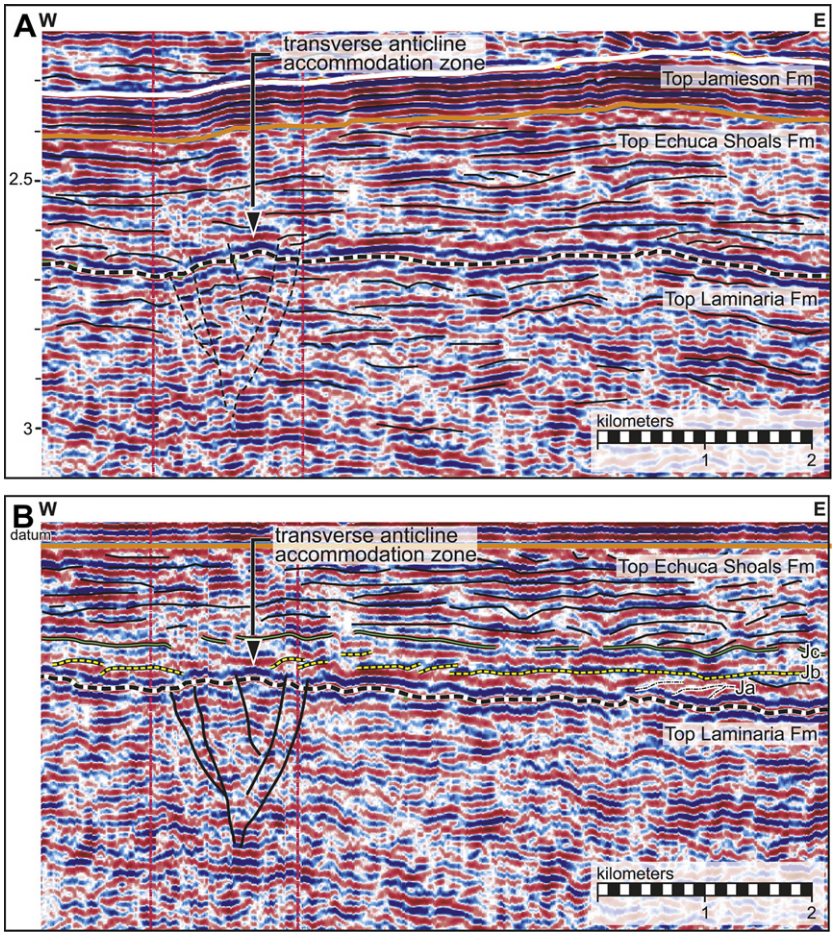

Fig. 5. E–W cross-section through the transverse anticline. Location on Fig. 4. (A) Seismic section with the top Laminaria Fm, top Echuca Shoals Fm and top Jamieson Fm. (B) Flattened seismic section and definition of the stratigraphic pattern above the top Laminaria Fm.

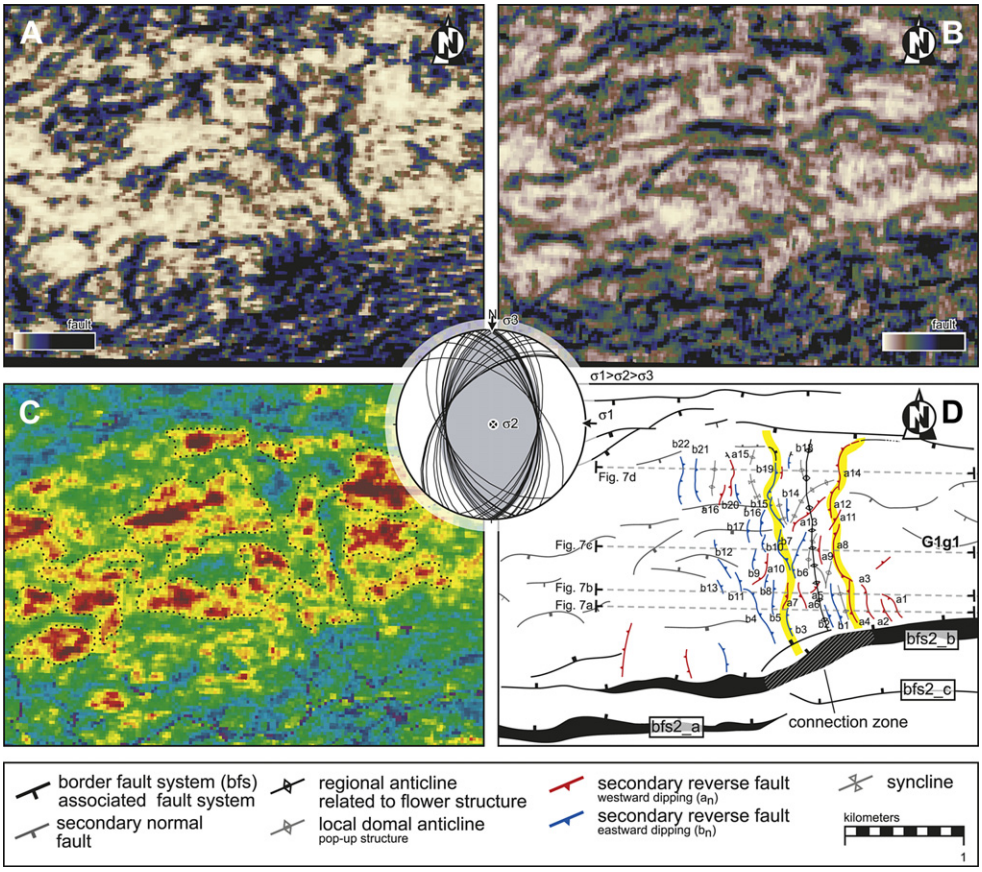

Fig. 6. Structure map of the flower structure on the western Laminaria High, top Laminaria Fm. Location on Fig. 4. (A) Variance extraction on top Laminaria Fm, on EW-trending variance cube (EW features are preferably highlighted in dark gray). (B) Variance extraction on top Laminaria Fm, on NS-trending Variance cube (NS features are preferably highlighted in dark gray). (C) Amplitude extraction, on top Laminaria Fm, on classic amplitude seismic data. Positive anomalies are highlighted by dashed lines with higher values in dark. (D) Structure map of the flower structure and the subtle EW-trending secondary faults. The local Late Jurassic stress field associated with the secondary flower structure is characteristic of a strike-slip regime with $\sigma_{hmax} > \sigma_v > \sigma_{hmin}$ ($\sigma_1 > \sigma_2 > \sigma_3$).

a near-sigmoidal pattern previously described by McClay and Bonora (2001) for similar modelled structures.

Despite the average seismic resolution, 53 segments have been identified within this structure and 37 of them intercept the Oxfordian top Laminaria Fm horizon (Fig. 6).

These segments are eastward and westward dipping with an average length of ca. 400 m (smallest interpreted segment = ca. 100 m, largest = ca. 550 m) and an average dip of 50°. They are NNW- to N-orientated, almost perpendicular to the principal structural trend and cross a 2 km wide associated graben (G1g1, Fig. 6). The flower structure is clearly related to a connection zone on the principal seaward dipping border fault (bfs2_b, Figs. 4 and 6) with its southern end located on the connecting segment between parent and tip faults (*connection zone* on Fig. 6). To the north, the structure tends to widen (up to 1.5 km wide) and then terminates against a landward dipping (southward dipping) fault system. In the vicinity of this northern limit, reverse faults can rapidly change to normal faults without variation of strike geometry (Fig. 6).

Beside the north-trending "regional" transverse anticline (Fig. 6) that defines the overall structure several local anticlines have been identified forming secondary pop-up structures (Fig. 7).

Calculated stress field state around the flower structure shows a local rotation of the constraints. The horizontal stresses remain similar to the regional ones with σ_{hmax} (σ_1) sub-parallel to the border fault system and σ_{hmax} (σ_3) sub-parallel to the extension direction and σ_v becoming the intermediate stress (σ_2) inducing a reverse setting (Fig. 6).

Serial cross-sections across the flower structure reveal its internal geometry (Fig. 7).

To the south (Fig. 7a) the structure is slightly asymmetric with the main pop-up structures shifted to the east (between a1-b2 and b1-b2, Figs. 6d and 7a). The pop-up structures are associated with concave up or planar reverse faults. Maximum reverse offset reaches ca. 12 ms TWT (ca. 15 m) and the elevation of the main pop-up structure relative to the average graben altitude is ca. 35 ms TWT (ca. 50 m).

Going northward, the flower structure regains symmetry (Fig. 7b) with a series of pop-ups forming a well-developed anticline (more than 1 km wide) between two principal divergent reverse faults (a1 and b4; Figs. 6d and 7b).

Near the centre of the graben (Fig. 7c), a narrow pop-up structure develops. Maximum reverse offset reaches ca. 15 ms TWT (ca. 20 m) and the elevation of the main structure relative to the average graben altitude is ca. 40 ms TWT (ca. 55 m). The overall flower structure is associated with concave up or planar reverse faults.

At the northern extremity (Fig. 7d), the widening of the overall structure is associated with the development of two distinct flower structures (between a14-b19 and a15-b22; Figs. 6d and 7d).

Rapid variations in geometry and dip direction of reverse faults are often recorded within the flower structure that forms the transverse anticline, such character is typical of a reverse fault system forming a flower structure in response to a strike-slip movement (Christie-Blick and Biddle, 1985).

5. Fault systems evolution

Transverse or oblique secondary structures, related to accommodation zones between principal border faults or to variation of

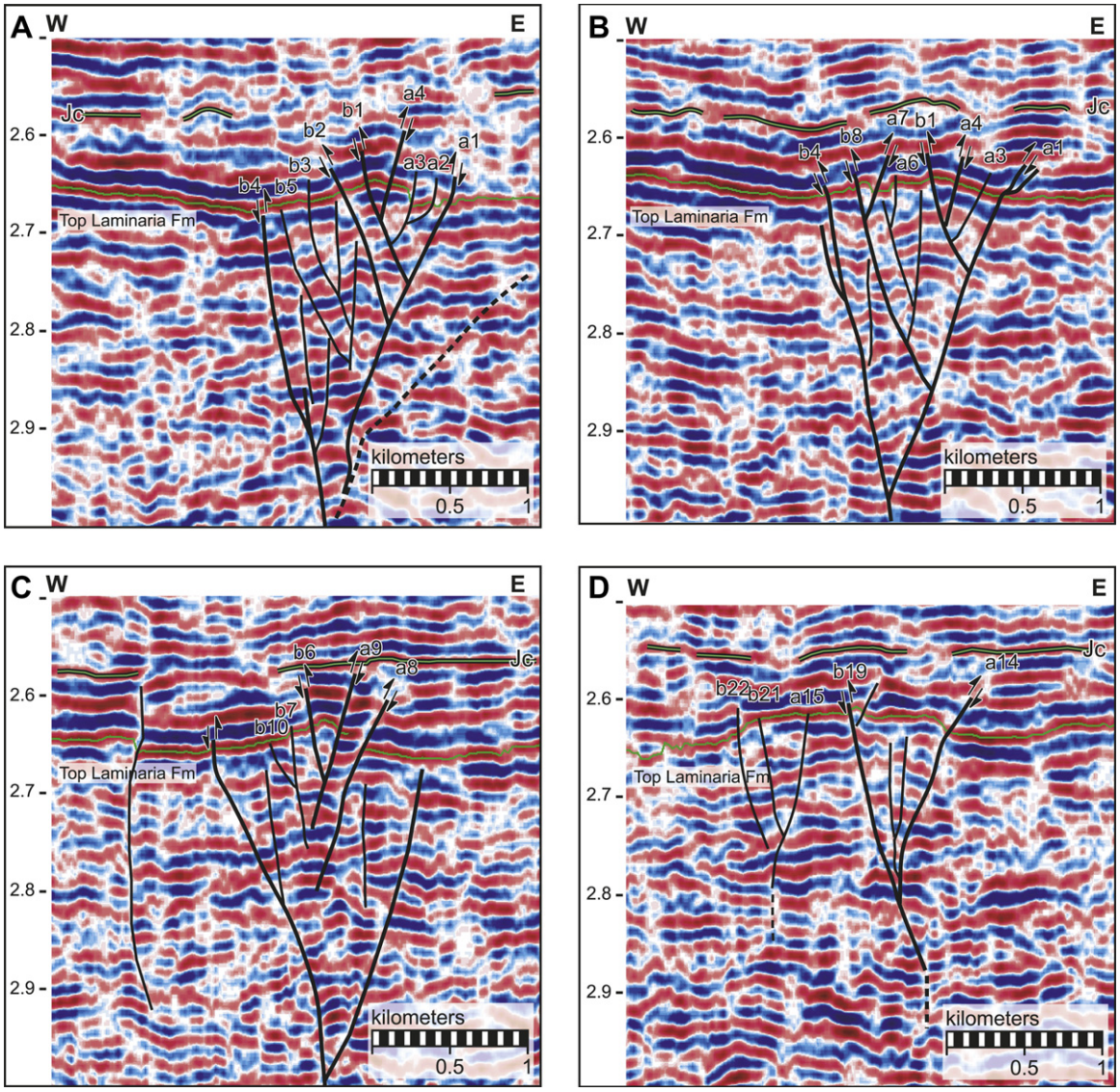

Fig. 7. Serial cross-sections across the flower structure. Location on Fig. 6.

geometry of a principal border fault plane, have long been recognised in extensional settings (e.g. Morley et al., 1990; Schlische, 1993; Polis et al., 2005). Secondary transverse anticlines and synclines can control the distribution of oil and gas accumulations by influencing the deposition of reservoir and source-rocks, by facilitating or restricting migration and by forming stratigraphic and structural traps (e.g. Morley et al., 1990; Gawthorpe and Hurst, 1993; Destro et al., 2003; Polis et al., 2005). Transverse anticlines have great potential for closure and concentration of hydrocarbons (Faulds and Varga, 1998).

The positive flower structure observed on seismic over the Laminaria High is clearly related to a connection zone between two segments of a border fault plane (bfs2_b, Figs. 4 and 6). Such connection zones can form either by interference between isolated faults ("isolated-to-isolated fault-linkage process" after Marchal et al., 2003) or, as here, the result of a "tip-to-parent connection" (Marchal et al., 2003). This occurs when a single fault plane grows by addition of secondary structures that step out of plane (laterally), to form unconnected tip faults and en-echelon patterns and then undulating zones (see Marchal et al., 2003).

The pattern formed by the border fault bfs2_b (Fig. 4) is characteristic of an isolated fault horizontal termination and reflects the tip-to-parent arrangement described by Marchal (1998) an Marchal et al. (2003). The composite nature of the border fault plane is represented by a bent segment that corresponds to a connection zone between parent and tip fault (Figs. 4 and 6). Furthermore, the border fault plane (i.e. bsf2_b in Fig. 4) displays associated features that are characteristic of grown single fault, such as incipient fault tips, breached relay ramp and a possible splay branch (Fig. 4) (see Fig. 4 in Marchal et al., 2003).

The throw variation for this fault plane (i.e. bsf2_b, Figs. 4 and 6) is presented on a displacement–distance plot in Fig. 8 (D–X graph in Muraoka and Kamata, 1983) and shows the along-strike vertical offset variation relative to the horizontal distance for the top Laminaria Fm. The zone of maximum throw (ca. 150 ms TWT or 200 m) is located on the eastern part of the fault plane and extends ca. 3 km westward from the point of maximum displacement (D_{max}, Fig. 8). West of the maximum displacement point, a lower displacement gradient is recorded (ca. 100–120 ms TWT or 150–160 m) until the fault reaches the connection zone (10–11 km from D_{max}). This area is characterised by minimum values of throw (ca. 60 ms TWT or 80 m), reflecting the presence of the positive flower structure. The local relative maximum throw of the western-most segment of the fault plane (tip fault) is less than 100 ms TWT (120–130 m).

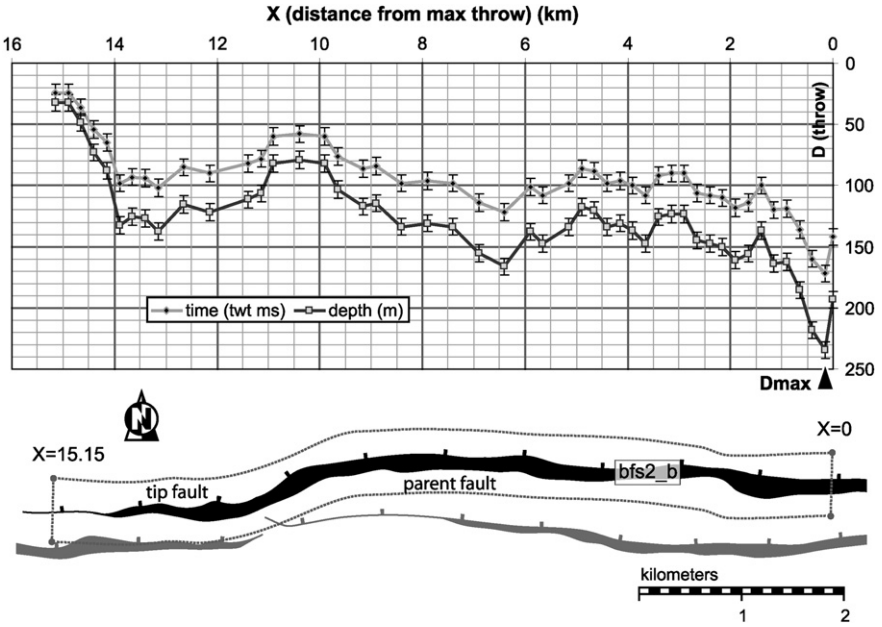

Fig. 8. Throw variation along the bfs2_b fault plane showing the along-strike vertical offset variation relative to the horizontal distance. Throw is shown in ms TWT (gray line) and m (black line). The maximum throw value for the bfs2_b fault plane is labelled D_{max}. The flower structure (transverse anticline) correlates with a minimum in throw values between 10 and 11 km from D_{max}. The parent fault is on the right side of the graph and the tip fault on the left side.

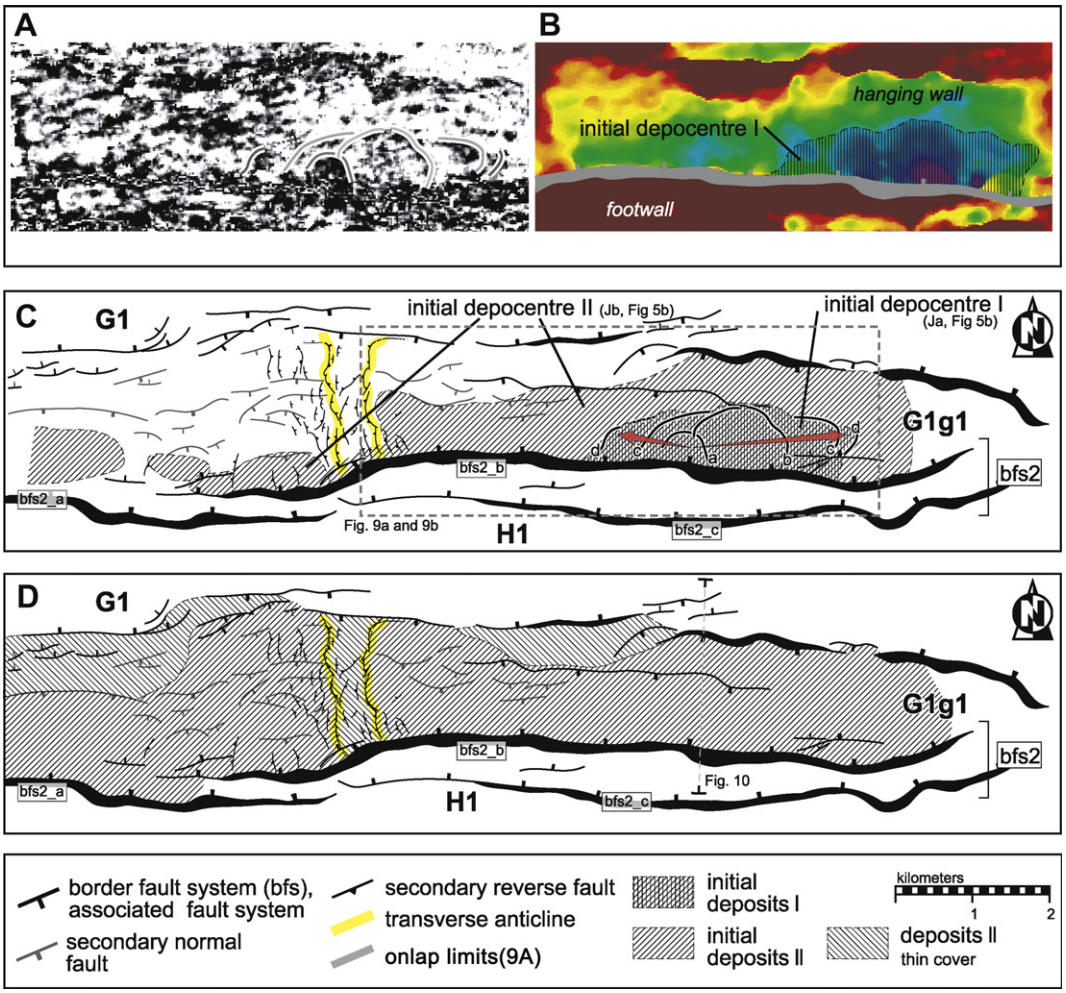

Fig. 9. Extension of the first deposits on the bsf2_b hanging-wall block. (A) Amplitude map 25 ms above top Laminaria Fm highlighting the geometry of the first onlap and the limits of the initial depocentre I. (B) Isopach map representing the paleotopography of the bfs2_b hanging-wall block. The initial depocentre I is correlated with the deepest area. (C) Sediments' extension for the initial depocentres I (reflectors Ja, Fig. 5b) and II (reflectors Jb, Fig. 5b). (D) Sediments' extension for the latest syn-rift phase (reflectors Jc, Fig. 5b).

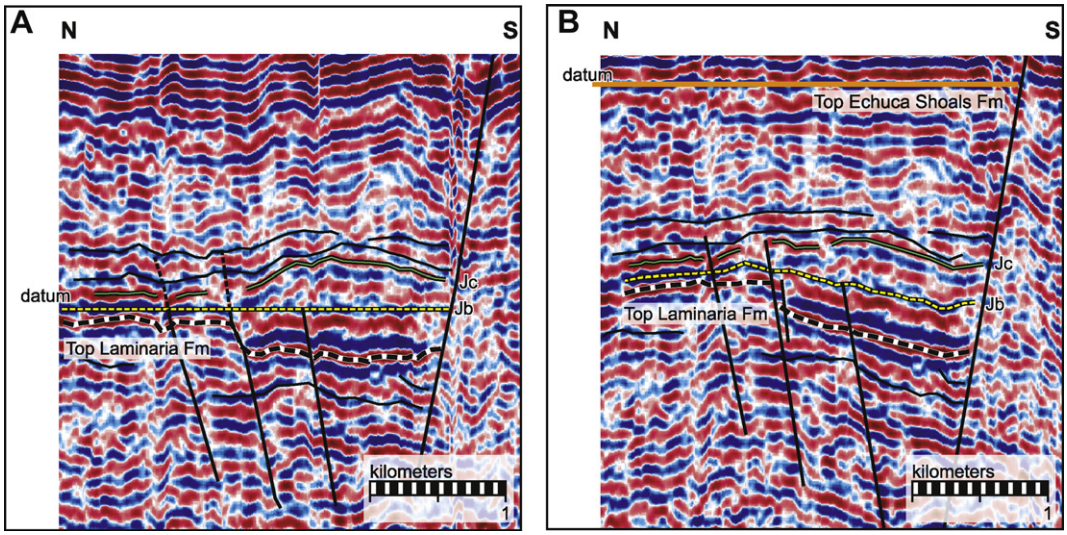

Fig. 10. N–S cross-section with syn-rift packages. Location on Fig. 9. (A) Seismic section flattened on Jb horizon. (B) Seismic section flattened on top Echuca Shoals Fm. Both sedimentary sections between top Laminaria Fm and Jb and between Jb and Jc show a thickening characteristic of syn-tectonic deposits.

The first sediments overlying the top Laminaria Fm (156 Ma, Fig. 2), and observable on the E–W section across the graben (Fig. 9), have been used to document the fault-linkage evolution and the coeval development of the flower structure.

The first deposits are located on the zone of maximum throw, with subtle onlap patterns visible on both the section (Fig. 5, reflectors Ja) and map view (Fig. 9a, c). These features define the limit of an initial depocentre (initial depocentre I, Fig. 9b, c) related to the development of the main border fault segment. During this early period, the western part of the main segment (3–10 km from D_{max} on Figs. 8 and 9c) may have potentially formed, but with offsets not significant enough to be associated with a sedimentary record definable on seismic data.

The architecture of the following Jb reflector, in-filling the restricted depocentres on both sides of the flower structure (initial depocentre II, Fig. 9c), suggests the quasi coeval development of the western part of the main segment and the tip fault, as well as the initiation of the transverse positive flower structure. This phase marks the connection of the border fault segments (parent and tip) and the initiation of the compartmentalization of the graben G1g1 (Fig. 4). Further to the west, as another border fault plane forms (bfs2_b, Fig. 9c), additional depocentres develop.

Once joined, the undulating border fault is still active as highlighted by the thickening of the sedimentary package between horizon Jb and Jc on the flattened cross-section (Fig. 10). The associated depocentre covers the entire restricted graben G1g1 (Fig. 9d) at this stage.

Following deposition of horizon Jc (Figs. 5 and 10), the relative constant thickness of overlying sedimentary packages (Fig. 10) suggests an important decrease in fault activity.

The Jc reflector also marks the cessation of the main activity of the flower structure (Fig. 7), highlighting the dependence between the two structures (i.e. bfs2_b and flower structure).

To further constrain the timing of the border fault and flower structure development, interpreted reflectors located in the G1 graben have been tied with stratigraphic markers from the footwall of the bsf2_b border fault (i.e. Alaria-1). While the top Laminaria Fm and post-rift markers (e.g. top Echuca Shoals Fm and top Jamieson Fm) correlate well through the border fault, the recognition of syn-rift horizons can be complicated by variations in their configuration between footwall and hanging wall.

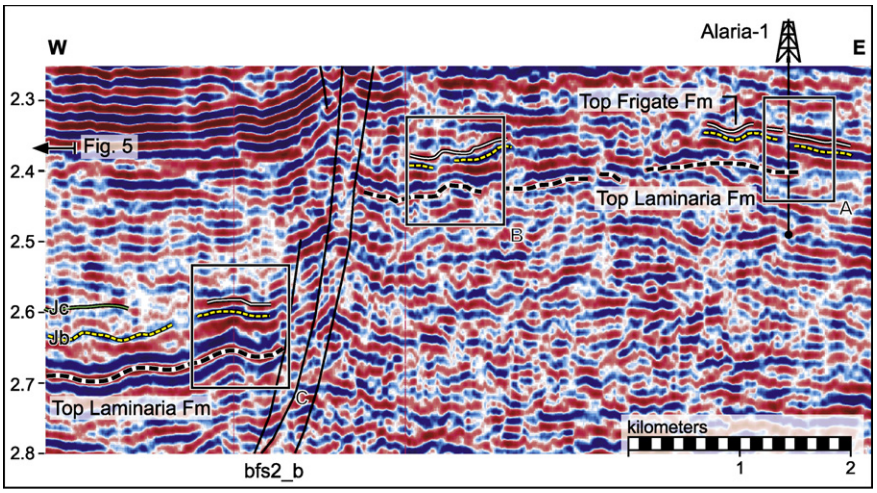

Fig. 11. Random cross-section from Alaria-1, located on the horst H1 trough the bsf2 fault system and to the graben G1. The seismic character of the top Frigate Fm in Alaria-1 (frame A) can be correlated eastward (frame B) and on the hanging-wall block (frame C). Location on Fig. 3.

In Alaria-1, the top of the Frigate Fm is characterised by the presence of a marly section (Iris Marl, ca. 152 Ma, de Ruig et al., 2000) associated with higher amplitude reflectors (Fig. 11).

Although this seismic character tends to vary and decrease laterally, it has been interpreted north of the border fault, within the graben G1, where it roughly corresponds to the Jc horizon (Fig. 11) and coeval with the decrease in fault activity.

Based on this interpretation, sedimentation rates (compacted and decompacted) have been calculated on the hanging wall of fault bfs2_b (Figs. 4 and 6), for the periods associated with the main tectonic activity and for the overlying section up to the Albian (Jamieson Fm).

While the Oxfordian–Kimmeridgian deposits (between top Laminaria Fm and Jc) show sedimentation rates of ca. 100 m/Ma (decompacted sediments), the rate for the overlying Tithonian–Albian section is only ca. 35 m/Ma (decompacted sediments).

This variation emphasizes the difference between an early Late Jurassic phase (Oxfordian–Kimmeridgian, top Laminaria Fm to Jc, i.e. Frigate Formation) of main tectonic activity, followed by a Late Jurassic to Cretaceous phase with decreasing tectonic activity and then finally with fault movement most likely associated with sediment loading.

6. Flower structure in extensional setting and effect of latter reactivation

The development of positive flower structures is commonly attributed to wrench or transpressional strike-slip zones (e.g. Christie-Blick and Biddle, 1985; Naylor et al., 1986; McClay and Bonora, 2001).

The displacement–distance plot for the fault bfs2_b (Fig. 8) shows displacement values higher for the western part of the main segment than for the tip fault. This element, associated with the left-stepping en-echelon pattern drawn by the segments (parent and tip, Figs. 12 and 13b), suggests a zone of differential displacement occurring between the two segments, at the location of an early accommodation zone. This configuration then allows for a local relative left-lateral strike-slip movement and transpressional uplift associated with restraining bend ("pop-ups and uplifts for restraining stepover geometry" in McClay and Bonora, 2001; Fig. 12).

During the Neogene time the Laminaria High has been affected by a tectonic phase induced by the complex collisional setting involving the irregular Australian northern margin, the Pacific plate and the Eurasian continent (Keep et al., 2002; Harrowfield et al., 2003). On the Laminaria High this phase reactivated the Late Jurassic structural features as demonstrated by the lateral distribution of the Neogene fault systems clustering above major underlying Mesozoic structures (Gartrell et al., 2006; Langhi, 2006). Most of the Neogene normal deformation is accommodated by Tertiary (Miocene–Pliocene) fault systems and therefore this episode does not appear to have significantly affected or modified the local Mesozoic structural style. The stratigraphic architecture of the Late Jurassic Formations (Figs. 5, 7 and 9) further emphasizes that the flower structure is clearly related to an Oxfordian–Kimmeridgian tectonic activity (between the top Laminaria Fm and reflector Jc, Fig. 7) as it post-dates the deposition of the Laminaria sandstone and pre-dates the deposition of the Flamingo Formation.

7. Conclusions

On the Laminaria High, the Late Jurassic (Oxfordian–Kimmeridgian) propagation of an E–W trending normal border fault was responsible for the development of a secondary local strike-slip setting and the formation of a N- to NNW-trending positive flower structure.

The development of such a secondary structure seems to be an isolated case as most observed fault zones in the area and in similar settings imply some degree of segments overlap and/or the development of splays that usually accommodate the differential

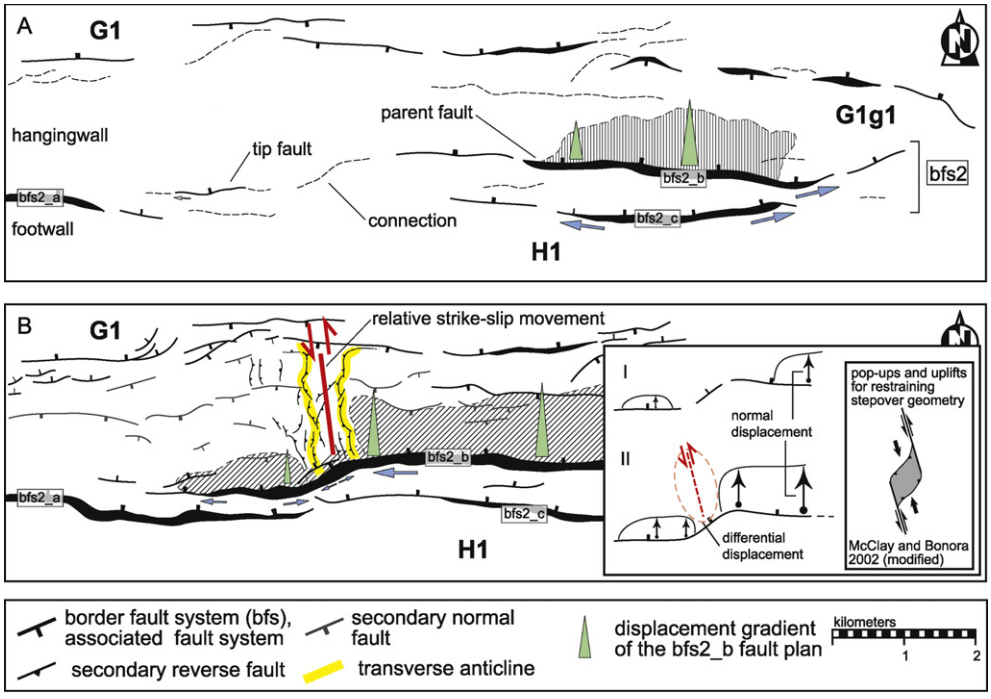

Fig. 12. Evolution of the bsf2_b fault and development of the flower structure. (A) Early stage of the Frigate Fm deposition and initiation of the bfs2 boundary fault system (deposition of Ja reflectors, Fig. 5b). (B) Development of a zone of differential displacement coeval with the connection of the bfs2_b parent and tip faults. The left-stepping pattern between the two fault segments and the variation of displacement gradient is responsible for the development of a relative left-lateral strike-slip movement. The secondary reverse structures are similar to pop-ups and uplifts for restraining stepover geometry modelled by McClay and Bonora (2001).

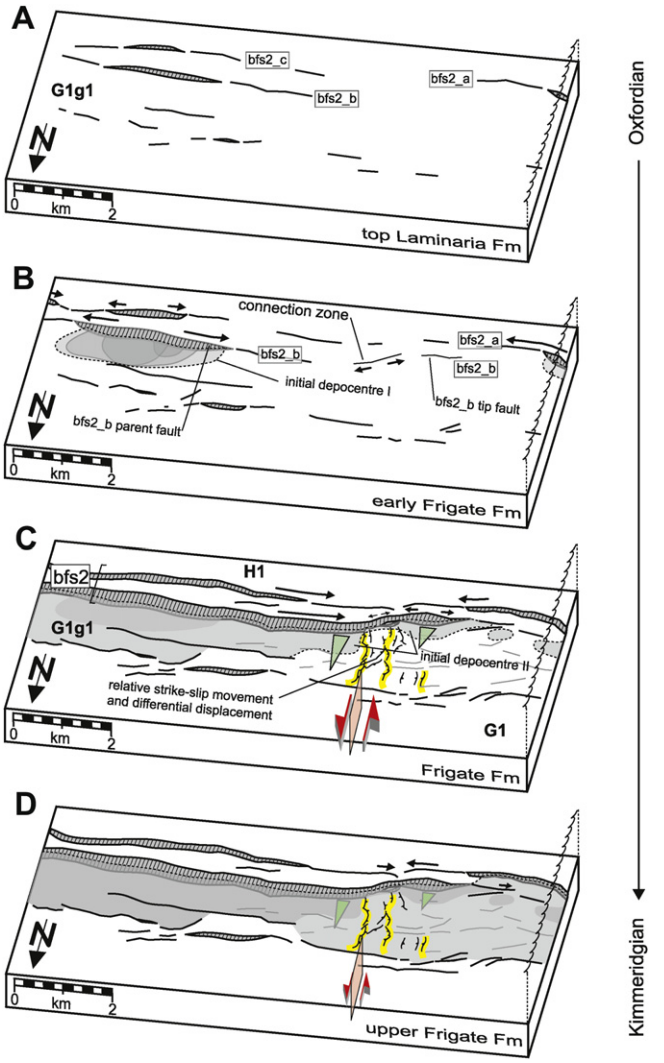

Fig. 13. Schematic block diagram with the evolution of the bfs2 fault and associated deposits. (A) Initiation of the fault system near the top Laminaria Fm (ca. 156 Ma). (B) Restricted early syn-rift deposits and development of the initial depocentre I during the early Frigate Fm. (C) Connection between bfs2_b parent and tip faults and development of strike-slip movement and the flower structure. (D) Following the connection, the bfs2_b fault plane is still active until the top of the Frigate Fm (ca. 152 Ma).

displacement and therefore prevent the development of oblique secondary reverse structures.

The Laminaria High the flower structure significantly affected the restricted graben G1g1 by controlling the sediments dynamics and the structural style. This structure, along with the associated secondary E–W trending system, has the potential to locally affect the trapping mechanism of fluids within the reservoir-prone Laminaria Fm as demonstrated by amplitude anomalies observed at the top of the sandstone unit.

It is observed as well that the positive flower structure directly affecting the oil-prone Oxfordian–Berriasian source-rock (Frigate Fm) could act as a migration barrier. Reduction of lateral conductivity due to the development of the reverse fault planes has the potential to jeopardise fluids transfer trough the G1g1 graben. These types of structure could be playing an important role in constraining the complex charge distribution pattern observed in the Laminaria High area where possible lack of adequate charge remains a major exploration risk.

The scenario where secondary positive structures develop and potentially affect the migration pathway supports the concept of compartmentalised source kitchens in the region as postulated by George et al. (2002).

Acknowledgments

The authors thank Woodside Energy Ltd for granting the access to the seismic data. We thank S. Reymond, C. Dyt, R. Kempton, A. Ross and an anonymous reviewer for their comments that improved the original manuscript. Schlumberger provided access to the GeoFrame software. This project has been partly supported by the Swiss National Fund for Research (SNF): grant number 2000-059188, 2000 20-100006/1.

References

AGSO, North West Shelf Study Group, 1994. Deep reflections on the north west shelf: changing perceptions of basin formation. In: Purcell, P.G., Purcell, R.R. (Eds.), The Sedimentary Basins of Western Australia: Proceedings of Petroleum Exploration Society of Australia Symposium. PESA, Perth, WA, pp. 63–76.

Baillie, P.W., Powell, C.M., Li, Z.X., Ryall, A.M., 1994. The tectonic framework of western Australia's Neoproterozoic to recent sedimentary basins. In: Purcell, P. G., Purcell, R.R. (Eds.), The Sedimentary Basins of Western Australia: Proceedings of Petroleum Exploration Society of Australia Symposium. PESA, Perth, WA, pp. 45–62.

Borel, G.D., 1997. Dynamique de l'extension mésozoique du domaine briançonnais: les Préalpes médianes au Lias. Doctoral thesis, University of Lausanne, Lausanne, 157 pp.

Borel, G.D., Stampfli, G.M., 2002. Geohistory of the NW Shelf: a tool to assess the Phanerozoic motion of the Australian Plate. In: Keep, M., Moss, S.J. (Eds.), The Sedimentary Basins of Western Australia 3. Proceedings of Petroleum Exploration Society of Australia Symposium. PESA, Perth, pp. 119–128.

Castillo, D.A., Bishop, D.J., Donaldson, I., Kuek, D., de Ruig, M.J., Trupp, M., Shuster, M. W., 2000. Trap integrity in the Laminaria High–Nancar Trough region, Timor Sea; prediction of fault seal failure using well-constrained stress tensors and fault surfaces interpreted from 3D seismic. APPEA Journal 40 (1), 151–173.

Christie-Blick, N., Biddle, K.T., 1985. Deformation and basin formation along strike-slip faults. In: Biddle Kevin, T., Christie Blick, N. (Eds.), Strike-slip Deformation, Basin Formation, and Sedimentation. Society of Economic Paleontologists and Mineralogists. SEPM (Society for Sedimentary Geology), Tulsa, OK, United States, pp. 1–34. Special Publication.

de Rooij, M., Tingdahl, K., 2002. Meta-attributes; the key to multivolume, multi-attribute interpretation. In: Eastwood John, E. (Ed.), The Attribute Explosion. Society of Exploration Geophysicists, Tulsa, OK, United States.

de Ruig, M.J., Trupp, M., Bishop, D.J., Kuek, D., Castillo, D.A., 2000. Fault architecture and the mechanics of fault reactivation in the Nancar Trough/Laminaria area of the Timor Sea, northern Australia. APPEA Journal 40 (1), 174–193.

Destro, N., Szatmari, P., Alkmim, F.F., Magnavita, L.P., 2003. Release faults, associated structures, and their control on petroleum trends in the Reconcavo Rift, Northeast Brazil. AAPG Bulletin 87 (7), 1123–1144.

Etheridge, M.A., O'Brien, G.W., 1994. Structural and tectonic evolution of the Western Australian margin rift system. Australian Petroleum Exploration Association Journal 34, 906–909.

Faulds, J.E., Varga, R.J., 1998. The role of accommodation zones and transfer zones in the regional segmentation of extended terranes. In: Faulds, J.E., Stewart, J.H. (Eds.), Accommodation Zones and Transfer Zones: the Regional Segmentation of the Basin and Range Province. Geological Society of America, Boulder, pp. 1–46. Special Paper.

Gartrell, A.P., Lisk, M., 2005. Potential new method for palaeostress estimation by combining 3D fault restoration and fault slip inversion techniques: first test on the Skua field, Timor Sea. In: Boult, P., Kaldi, J.K. (Eds.), Evaluating Fault and Cap Rock Seals. AAPG Hedberg Series, vol. 2, pp. 23–36.

Gartrell, A., Bailey, W.R., Brincat, M., 2006. A new model for assessing trap integrity and oil preservation risks associated with postrift fault reactivation in the Timor Sea. AAPG Bulletin 90 (12), 1921–1944.

Gawthorpe, R.L., Hurst, J.M., 1993. Transfer zones in extensional basins; their structural style and influence on drainage development and stratigraphy. Journal of the Geological Society of London 150 (6), 1137–1152.

George, S.C., Lisk, M., Eadington, P.J., Quezada, R.A., 2002. Evidence for an early, marine-sourced oil charge to the Bayu gas-condensate field, Timor Sea. In: Keep, M., Moss, S.J. (Eds.), The Sedimentary Basins of Western Australia 3. Proceedings of Petroleum Exploration Society of Australia Symposium. PESA, Perth, WA, pp. 465–474.

Harrowfield, M., Cunneen, J., Keep, M., Crowe, W., 2003. Early-stage orogenesis in the Timor Sea region, NW Australia. Journal of the Geological Society of London 160 (6), 991–1001.

Hocking, R.M., Mory, A.J., Williams, I.R., 1994. An atlas of Neoproterozoic and Phanerozoic basins of Western Australia. In: Purcell, P.G., Purcell, R.R. (Eds.), The Sedimentary Basins of Western Australia: Proceedings of Petroleum Exploration Society of Australia Symposium. PESA, Perth, WA, pp. 21–43.

Keep, M., Clough, M., Langhi, L., 2002. Neogene tectonic and structural evolution of the Timor Sea region, NW Australia. In: Keep, M., Moss, S.J. (Eds.), The

Sedimentary Basins of Western Australia 3. Proceedings of Petroleum Exploration Society of Australia Symposium. PESA, Perth, pp. 341–353.
Labutis, V.R., Ruddock, A.D., Calcraft, A.P., 1998. Stratigraphy of the Sahul Platform. APPEA Journal 38 (1), 115–136.
Langhi, L., 2006. 3D seismic facies characterisation and geological patterns recognition (Australian North West Shelf). Doctorat thesis, University of Lausanne, Lausanne, 197 pp.
Langhi, L., Borel, G.D., 2005. Influence of the Neotethys rifting on the development of the Dampier sub-basin (North West Shelf of Australia), highlighted by subsidence modelling. Tectonophysics 397 (1–2), 93–111.
Langhi, L., Reymond, S.B., 2005. Seismic attributes mapping of Late Palaeozoic glacial deposits on the Australian Northwest Shelf. Exploration Geophysics (Melbourne) 36, 224–233.
Longley, I.M., Buessenschuett, C., Clydsdale, L., Cubitt, C.J., Davis, R.C., Johnson, M.K., Marshall, N.M., Murray, A.P., Somerville, R., Spry, T.B., Thompson, N.B., 2002. The North West shelf of Australia – a woodside perspective. In: Keep, M., Moss, S.J. (Eds.), The Sedimentary Basins of Western Australia 3. Proceedings of Petroleum Exploration Society of Australia Symposium. PESA, Perth, WA, pp. 27–88.
Marchal, D., 1998. Approche spatio-temporelle des mécanismes de la propagation des failles normales: des modélisations analogiques à la sismique 3D. PhD thesis, Henry Poincarré, Nancy.
Marchal, D., Guiraud, M., Rives, T., 2003. Geometric and morphologic evolution of normal fault planes and traces from 2D to 4D data. Journal of Structural Geology 25 (1), 135–158.
McClay, K., Bonora, M., 2001. Analog models of restraining stepovers in strike-slip fault systems. AAPG Bulletin 85 (2), 233–260.
Morley, C.K., 2002. Evolution of large normal faults; evidence from seismic reflection data. In: Underhill John, R., Trudgill Bruce, D. (Eds.), The Structure and Stratigraphy of Rift Systems. American Association of Petroleum Geologists, Tulsa, OK, United States.
Morley, C.K., Nelson, R.A., Patton, T.L., Munn, S.G., 1990. Transfer zones in the East African Rift system and their relevance to hydrocarbon exploration in rifts. AAPG Bulletin 74 (8), 1234–1253.
Moustafa, A.R., 2002. Controls on the geometry of transfer zones in the Suez Rift and Northwest Red Sea; implications for the structural geometry of rift systems. In: Underhill John, R., Trudgill Bruce, D. (Eds.), The Structure and Stratigraphy of Rift Systems. American Association of Petroleum Geologists, Tulsa, OK, United States.
Müller, R.D., Mihut, D., Baldwin, S., 1998. A new kinematic model for the formation and evolution of the West and Northwest Australian margin. In: Purcell, P.G., Purcell, R. R. (Eds.), The Sedimentary Basins of Western Australia 2: Proceedings of Petroleum Exploration Society of Australia Symposium. PESA, Perth, WA, pp. 55–72.
Muraoka, H., Kamata, H., 1983. Displacement distribution along minor fault traces. Journal of Structural Geology 5 (5), 483–495.
Naylor, M.A., Mandl, G., Sijpesteijn, C.H.K., 1986. Fault geometries in basement-induced wrench faulting under different initial stress states. Journal of Structural Geology 8 (7), 737–752.
O'Brien, G.W., Higgins, R., Symonds, P., Quaife, P., Colwell, J., Blevin, J., 1996. Basement control on the development of extensional systems in Australia's Timor Sea: an example of hybrid hard linked/soft linked faulting? APPEA Journal 36, 161–200.
O'Brien, G.W., Lisk, M., Duddy, I.R., Hamilton, J., Woods, P., Cowley, R., 1999. Plate convergence, foreland development and fault reactivation; primary controls on brine migration, thermal histories and trap breach in the Timor Sea, Australia. In: Worden, R. (Ed.), Thematic Set on Geofluids. Marine and Petroleum Geology, 533–560. Elsevier, Oxford, United Kingdom.
Pattillo, J., Nicholls, P.J., 1990. A tectonostratigraphic framework for the Vulcan Graben, Timor Sea region. APEA Conference; Technical Papers. In: Barnes, D. (Ed.), Frontiers for the 1990s. APEA Journal, 27–51. Australian Petroleum Exploration Association, Sydney, N.S.W., Australia.
Polis, S.R., et al., 2005. Preferential deposition and preservation of structurally-controlled synrift reservoirs; northeast Red Sea and Gulf of Suez. GeoArabia (Manama) 10 (1), 97–124.
Reymond, S.B., 2000. New seismic methods and potential for the region. APPEA Journal 40, 326–340.
Schlische, R.W., 1993. Anatomy and evolution of the Triassic–Jurassic continental rift system, eastern North America. Tectonics 12 (4), 1026–1042.
Shuster, M.W., Eaton, S., Wakefield, L.L., Kloosterman, H.J., 1998. Neogene tectonics, Greater Timor Sea, offshore Australia: implications for trap risk. APPEA Journal 38 (1), 351–379.
Smith, G.C., Tilbury, L.A., Chatfield, A., Senycia, P., Thompson, N., 1996. Laminaria – a new Timor sea discovery. APPEA Journal 36 (1), 12–28.
Stampfli, G.M., Borel, G.D., 2002. A Plate tectonic model for the Paleozoic and Mesozoic constrained by dynamic plate boundaries and restored synthetic oceanic isochrons. Earth and Planetary Science Letters 196 (1–2), 17–33.
Stone, D.S., 1995. Structure and kinematic genesis of the Quealy wrench duplex: transpressional reactivation of the Precambrian Cheyenne belt in the Laramie basin. Wyoming. AAPG Bulletin 79, 1349–1376.
Veevers, J.J., 1988. Morphotectonics of Australia's northwestern margin – a review. In: Purcell, P.G., Purcell, R.R. (Eds.), The North West Shelf of Australia. Proceedings of Petroleum Exploration Society of Australia Symposium. PESA, Perth, WA, pp. 19–27.
Whittam, D.B., Norvick, M.S., McIntyre, C.L., 1996. Mesozoic and Cenozoic tectonostratigraphy of Western Zoca and adjacent areas. APPEA Journal 36 (1), 209–231.
Yeates, A.N., et al., 1987. The Westralian Superbasin: an Australian link with Tethys. In: McKenzie, K.G. (Ed.), Shallow Tethys, vol. 2. A.A. Balkema, Rotterdam, Netherlands, pp. 199–213.